

## Environmental and economic assessment of ITO-free electrodes for organic solar cells

Christopher J.M. Emmott<sup>a,\*</sup>, Antonio Urbina<sup>a,b</sup>, Jenny Nelson<sup>a</sup>

<sup>a</sup> Department of Physics and Grantham Institute for Climate Change, Imperial College London, London SW7 2AZ, United Kingdom

<sup>b</sup> Department of Electronics, Technical University of Cartagena, Plaza Hospital 1, 30202 Cartagena, Spain

### ARTICLE INFO

#### Article history:

Received 1 July 2011

Received in revised form

7 September 2011

Accepted 12 September 2011

Available online 5 October 2011

#### Keywords:

Organic photovoltaics

Polymer solar cells

Life cycle analysis

Economic analysis

ITO-free

Transparent conductors

### ABSTRACT

The use of Indium–Tin Oxide (ITO) as a transparent conductor in organic photovoltaic (OPV) devices has been shown to present a bottleneck for the technology due to the use of the rare metal Indium and also the energy intensive manufacturing processes required and subsequent high economic cost. This study discusses some of the alternative materials, which are being considered for use as transparent conductors in OPV modules. A life cycle and cost analysis of a number of the most promising ITO-free transparent conductors, namely: high conductivity PEDOT:PSS; a silver grid embedded in PEDOT:PSS; silver nanowires; single walled carbon nanotubes are completed in this study. The results show that there is great potential for reducing both the energy pay-back time and the cost of OPV modules by replacing ITO with an alternative transparent conductor.

© 2011 Elsevier B.V. All rights reserved.

### 1. Introduction

Organic photovoltaics (OPV) are often cited as being a low cost, low embodied energy route to photovoltaic electricity. However, the use of Indium Tin Oxide (ITO) as a transparent conductor (TC) limits the degree to which costs and embodied energy can be reduced by adopting OPV technology [1–4]. The ITO electrode is fabricated via a vacuum sputtering process, which is extremely energy intensive<sup>1</sup> and economically expensive, thus contributing a large amount to both the economic cost and Energy Payback Time (EPBT) of OPV modules [7,8]. In addition there is the potential for a bottleneck in the scale-up of OPV due to the use of the scarce element, Indium [9]. Moreover, the use of ITO also limits the robustness of device performance under flexing [10].

**Abbreviations:** TC, Transparent Conductor; OPV, Organic Photovoltaics; ITO, Indium–Tin Oxide; SWCNT, Single-Walled Carbon Nanotube; AgNW, Silver Nanowire; CVD, Chemical Vapour Deposition; VPP, Vapour Phase Polymerisation; HC-PEDOT:PSS, High Conductivity PEDOT:PSS; LCA, Life Cycle Analysis; LCI, Life Cycle Inventory; EPBT, Energy Payback Time; PR, Performance Ratio.

\* Corresponding author at: Imperial College London, Department of Physics, Blackett Laboratory, Prince Consort Road, London, SW7 2BW, United Kingdom. Tel.: +44 2075947563; fax: +44 207 594 2077.

E-mail address: christopher.emmott@imperial.ac.uk (C.J.M. Emmott).

<sup>1</sup> There exists some discrepancy in the amount of energy involved in the sputtering processes when one compares published calculations and some databases [5,6]; however, there is general agreement that ITO accounts for the largest share of the embodied energy in OPVs.

Numerous alternative TCs have been explored in order to avoid the use of ITO as the transparent conducting electrode in organic photovoltaics. Such alternatives have the potential to alter device performance via changes to the series resistance across the device, lower transparency leading to lower photogenerated current and effects on the lifetime. However, any detrimental effects could be tolerated if the overall cost or energy requirements for manufacture of OPV modules were significantly reduced. The converse of this has previously been observed in the use of novel active layers to fabricate more efficient devices, which have been seen to adversely affect the EPBT of the device [11].

A number of life cycle analysis (LCA) studies have analysed OPV modules, as well as their use in specific applications [5,7,12–14]. This article presents a life cycle and cost analysis of OPV devices manufactured using an existing process but with ITO-free electrodes in place of ITO, making use of data gathered during previous studies [7,8]. We calculate an EPBT and cost per Watt for OPV modules for each alternative TC considered.

This paper is organised as follows. Section 2 presents a range of TCs, which have been studied in the literature, and discusses their potential for reducing the cost and EPBT of OPV modules. Section 3 presents a life cycle analysis of four of the most promising ITO-free TCs, namely: high conductivity PEDOT:PSS; a silver grid embedded in PEDOT:PSS; silver nanowires; single walled carbon nanotubes, whilst Section 4 presents a cost analysis of the same TCs. Section 5 discusses the effect that replacement of the TC may have on the performance of the device and presents a method for theoretically calculating such an effect. Finally, Section 6 concludes and summarises the findings of this study.

**Table 1**  
Best demonstrated performance results of TCs on flexible substrates.

Film type	Sheet resistance ( $\Omega/\text{sq}$ )	Transparency (%)	Reference
Sputtered ITO <sup>a</sup>	60	79	[15]
HC-PEDOT:PSS	63.3	67.4	[16]
VPP-PEDOT	130	~80	[17]
Metal grid embedded in PEDOT:PSS	1 <sup>b</sup>	92	[18]
Metal nanogrid	23	80	[19]
Metal nanowires	8	80	[20,21]
SWCNTs	40	70	[22]
CVD graphene	~30	~90	[23]
Reduced graphene oxide	80	79	[24]

<sup>a</sup> Characteristics shown here are for the most commonly used ITO on PET, rather than the best demonstrated performance film.

<sup>b</sup> Sheet resistance shown here is for the metal grid only rather than the composite film.

## 2. Transparent conductors in organic solar cells

Candidates for ITO-free TCs include: semitransparent or patterned metal layers; doped metal oxides; conductive polymers; metal nanowires; carbon nanotubes; graphene among others. OPV devices require an electrode with a number of key properties including high transparency, good conductivity and low surface roughness. The degree to which a TC possesses these properties can greatly affect the performance of an OPV device. Table 1 shows the best published results for various TCs on flexible substrates.

### 2.1. Conductive polymers

The use of conductive polymers shows a promising method for fabricating alternative TCs. Poly(3,4-ethylenedioxythiophene) is often combined with poly(styrenesulfonate) (PEDOT:PSS) in order to enable aqueous solubility and thus allow solution processing of the layer; however, the addition of PSS reduces the conductivity of the PEDOT [25]. PEDOT:PSS modified by the addition of highly dielectric solvents such as DMSO, ethylene glycol or diethylene glycol is known to greatly increase the conductivity of a PEDOT:PSS film [26]. These additives make PEDOT-rich chains, which increase the conductivity of the film [27]. Subsequently, a number of companies (namely HC-Stark and Agfa-Gevaert N.V.) have begun to manufacture solutions of high conductivity PEDOT:PSS (HC-PEDOT:PSS) capable of reaching low sheet resistances and these formulations have been used as TCs in OPV devices [16,28–35].

One method of fabricating PEDOT films without the addition of PSS is by vapour phase polymerisation (VPP) of 3,4-ethylenedioxythiophene (EDOT), which leads to a promising TC [25,36]. Unfortunately, lack of information of a scalable example of such a process prevented the completion of an LCA of this material for this study.

### 2.2. Metallic grids

Large scale grids (on the millimetre scale), either evaporated or screen printed from a metallic ink have been investigated in order to increase the conductivity of PEDOT:PSS [18,37–40]. The best results of a metal grid embedded in PEDOT:PSS [39] have used a very thin PEDOT:PSS layer and thermal evaporation to deposit the grid. This is a very energy intensive process [5] and so this study instead analyses the more promising solution of a screen printed grid. However, it has been observed that a very thick layer of PEDOT:PSS is required since otherwise solvent within the silver

ink seeps into the active layer, and this thickness results in poor performance due to low transparency [38].

Nanoscale grids have been fabricated via nanoimprint lithography of a metal layer [19,41–43]. However, this process involves printing the nanogrid from a PDMS stamp, which has been coated in the metal, usually via thermal or e-beam evaporation, which are extremely energy intensive processes [5].

### 2.3. Nanowires and nanotubes

Silver nanowires represent an alternative method for creating a transparent metallic coating, which can be produced by solution processable methods and have the potential for being a low cost and low energy alternative to sputtered or thermally evaporated metal films [20,21,44–47]. Silver nanowires are fabricated by reduction of silver nitride to create a functional ink, which can be deposited by low cost and low energy processes such as slot-die or spray coating [44]. The performance of such films is dramatically improved by coating of the nanowires in gold via galvanic displacement, which greatly reduces the resistance of the junctions between nanowires [20].

In the same way as for metal nanowires, single-walled carbon nanotube (SWCNT) TCs can be produced by spray coating a solution of SWCNTs onto a transparent substrate. An ink is prepared by creating an aqueous solution of SWCNTs with the addition of a surfactant [48]. This can then be deposited by a variety of methods onto a prepared substrate. The film is finally washed with acid, which improves conductivity due to the removal of excess surfactant and the subsequent film densification, which acts to decrease the resistance across junctions between SWCNTs and enhances the metallicity of the SWCNTs [22]. Both nanowires and nanotubes present a promising ITO-free TC; however, both have a number of issues regarding the roughness of the resulting film as well as their adhesion to the substrate.

### 2.4. Other materials

Other transparent conducting oxides (TCOs), manufactured similar to ITO, such as Fluorine-doped tin oxide and Gallium-doped Zinc Oxide, have been used in polymer electronic devices [10,49]. However, analysis has shown that by replacing ITO with other sputtered metals does not avoid the issue of the high energy intensity of this layer [13]. Most methods used to deposit unpatterned, monolithic, transparent metal layers currently require very energy intensive processes, often in vacuum or high temperature conditions, such as sputtering and thermal evaporation [49–53], and thus do not appear to be a promising solution to the high energy intensity of TC fabrication.

Graphene films are often cited as being a potentially excellent replacement to ITO [3,4,54]. The most common and successful method for creating highly conductive graphene films is by chemical vapour deposition (CVD) onto a variety of metallic substrates, which are then transferred onto transparent substrates to create a TC [23,54–60]. However, CVD is a very energy intensive process, which accounts for the vast majority of the embedded energy in amorphous silicon solar modules [61]. Thus, although CVD graphene may be able to achieve excellent performance attributes, good flexibility and a high potential for low cost [54], it fails to solve the problem of the high embedded energy of ITO (assuming that the conditions for CVD of amorphous silicon are similar to that for graphene). Although an alternative method for graphene production from solution has been published [24,62,63], an LCA of this method could not be completed due to a lack of information in the literature.

This study provides a detailed life cycle and cost analysis of four, solution processable, TCs: high conductivity PEDOT:PSS

(HC-PEDOT:PSS); a silver grid embedded in PEDOT:PSS; silver nanowires (AgNWs); single walled carbon nanotubes (SWCNTs). These materials were chosen due to their potential for low cost and low energy manufacture, as well as the availability of detailed information of their manufacture.

### 3. Life cycle analysis

In order to carry out a LCA of modules based on alternative TCs, we use the data and methodology from a previous LCA of a pre-industrial roll-to-roll manufacturing process for OPV modules, known as ProcessOne [7], where we replace the ITO with each of the selected TCs.

Here we account for the embedded energy in all raw materials used in the fabrication of the TC as well as the energy requirements for manufacture. Energy demands associated with the manufacture of the required equipment as well as transport of the raw materials and the final product are not included in this analysis. From a detailed life cycle inventory (LCI), gathered for the various TCs, the embodied energy of the raw materials was found and electricity requirements were converted to equivalent primary energy using a 35% conversion factor.

ProcessOne is based on the following cell architecture: ITO/ZnO/P3HT:PCBM/PEDOT:PSS/Ag. Fig. 1 shows the contribution of the various TCs to the embodied energy in the module. Fig. 3a shows a comparison of the effect using different TCs to replace ITO in this architecture has on the EPBT of the module. The EPBT calculation is based on a cell efficiency of 3%, a performance ratio (PR) of 75% to account for system losses, a photovoltaically active area of the module of 67% and annual insolation of 1700 kWh/m<sup>2</sup>, which is typical of Southern Europe.

#### 3.1. High conductivity PEDOT:PSS

A process for creating HC-PEDOT:PSS films via slot-die (S-D) coating was analysed. The HC-PEDOT:PSS ink was assumed to be comprised of conventional PEDOT:PSS with the addition of 5% DSMO or ethylene glycol. Commercial HC-PEDOT is likely to contain small amounts of unknown additives; however, since conventional PEDOT:PSS has a high embodied energy, it can be assumed that any small amount of additive would contribute a negligible amount to the embodied energy in the layer. Since the best results for HC-PEDOT:PSS films in the literature consist of very thin coatings (around 200 nm [16]), the S-D coating conditions were based on similar coating thicknesses used in the manufacture of ProcessOne modules (i.e. for the ZnO and active layers), for which a detailed LCA has already been completed [7].

The LCA of HC-PEDOT:PSS shows that this layer has an extremely low embodied energy in comparison to the rest of the module, see Fig. 1. The largest contributions to the embedded

energy within this layer are due to the electricity required to S-D coat and dry the layer, which contribute around 75% of the embedded energy. The remainder is largely accounted for by the energy embedded in the Isopropanol used to wash the substrate before the HC-PEDOT:PSS is applied. Less than 1% of the embedded energy is due to the embedded energy in the HC-PEDOT:PSS.

#### 3.2. PEDOT:PSS with silver grid

A life cycle analysis of a silver grid embedded in PEDOT:PSS is completed, in this study, based on an adapted ProcessOne, known as ProcessTwo [38]. ProcessTwo replaced the ITO used in ProcessOne with a screen printed silver electrode, and altered the top silver electrode to a grid pattern. A life cycle analysis of a similar module, known as HIFLEX (which contains a sputtered Aluminium and Chromium layer), which also employs the use of such a silver grid TC, has been completed in a previous study [13]. The data collected during this study for the silver grid and PEDOT:PSS composite TC were used in this study to allow a comparative analysis of this TC.

The embodied energy in the composite silver grid and PEDOT:PSS TC was largely accounted for equally by the drying of the PEDOT:PSS and the electricity required for screen printing, which represent 77% of the embodied energy in the TC. The large contribution due to the energy for PEDOT:PSS drying is the result of a need for a thick layer to prevent damage to the active layers due to solvents in the silver ink, as mentioned above (see Section 2.2).

#### 3.3. Silver nanowires

In order to complete the LCA of a silver nanowire (AgNW) film, a life cycle inventory of AgNW ink given in [20] was combined with the energy requirements for slot-die coating of the PEDOT:PSS layer in ProcessOne [7], since the wet film thickness and drying conditions are similar for these two layers. The results of this analysis showed that processing AgNW film requires little energy compared to ITO, see Table 2.

The AgNW are highly dispersed in the ink used to create these TCs, thus a thick layer of ink is required in the fabrication process [20]. The resulting energy required in S-D coating and drying of this layer subsequently account for approximately 55% of the embodied energy in the film. The remaining embodied energy is mostly attributed to the embodied energy in the raw materials, in particular to ethylene glycol, which is used as a solvent.

#### 3.4. Carbon nanotubes

A life cycle analysis of a process for creating SWCNT films via spray deposition for use in OPV devices [48] was completed in this study.

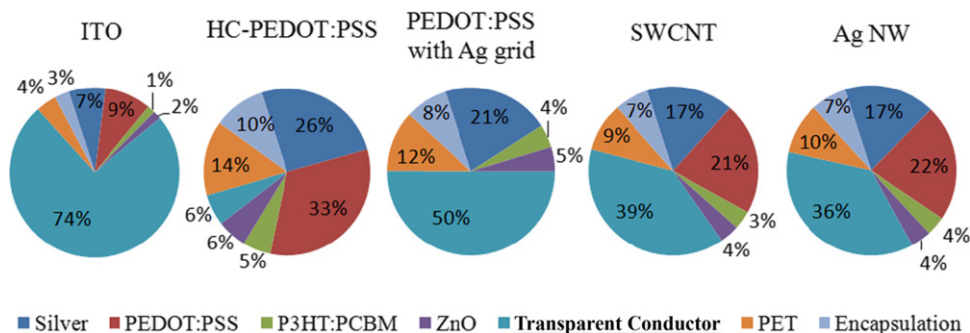


Fig. 1. Pie charts showing the breakdown of the maximum energy embedded in modules using various TCs.

The best performing SWCNTs, which are created via arc-discharge [64], are extremely energy intensive to manufacture, with an embedded energy of 6523 MJ/kg [65]. However, the small amount of carbon nanotubes required (despite this study finding this amount to be much larger than has previously been suggested [66,67], see Section 4.4) mean that their embedded energy contributes around 5% of the total energy embedded in the film. The SWCNT ink used in this process contains only 0.03% carbon nanotubes [48], thus the wet layer of the spray coated ink is extremely thick and subsequently requires an extensive drying time.

#### 4. Economic cost analysis

To calculate the cost of modules, a published cost model [8] was extended using data gathered for the TCs shown above. Details of the life cycle inventory and material costs for the TCs can be found in the supplementary information, and are summarised in Table 2. Labour costs and the capital costs of required machinery for TC manufacture (with the exception of ITO) were not included as they were expected to be small [8].

Labour, overheads and investment costs associated with all layers in the modules except the TC, as found in [8], were included at a minimum value of 20.05 €/m<sup>2</sup>, and a maximum value of 28.23 €/m<sup>2</sup>. Subsequently, the cost per Watt of ITO-free modules was calculated, using the same assumptions for cell efficiency, PR, active area and insolation as for the LCA calculations, and is presented in Fig. 4a. Fig. 2 shows the contribution of the various TCs to the cost of the module.

##### 4.1. High conductivity PEDOT:PSS

A cost analysis of a HC-PEDOT:PSS film was completed based on the price of commercially available HC-PEDOT:PSS along with

**Table 2**

Summary of LCA and cost analysis results for various TCs, from this study unless otherwise noted. Note that these values do not contain the embodied energy or cost of the PET substrate with the exception of the cost of ITO film which contains the cost of PET.

Transparent conductor	Embodied energy (MJ EPE/m <sup>2</sup> )		Cost (Euro/m <sup>2</sup> )	
	Min	Max	Min	Max
ITO	71.98 [6]	271.19 [7]	14.64 [8]	65.50 [8]
HC-PEDOT:PSS	5.61	6.03	0.11	1.27
PEDOT:PSS with Ag grid	61.24	62.03	19.57	21.17
Ag nanowires	47.84	53.78	5.31	17.87
SWCNTs	57.41	59.48	102.66	339.58

the electricity requirements for the S-D coating of such a film. The cost of the HC-PEDOT:PSS accounted for between 30% and 50% of the cost of the TC, with Isopropanol, which is used for preparing the substrate, accounting for the majority of the remaining cost.

##### 4.2. PEDOT:PSS with silver grid

The cost analysis of a silver grid embedded in PEDOT:PSS found that the thick layer of PEDOT:PSS required in the process analysed, ProcessTwo, along with the silver ink, account for 98% of the cost of such a film. However, it should be noted that when extending this analysis to the module level, the PEDOT:PSS layer within the module is already accounted for, as can be seen in the cell architecture of ProcessTwo [38]. Subsequently, a direct comparison of the cost of this TC with other alternatives, as shown in Table 2, overestimates the impact this has on the module level, which is shown in Fig. 2.

##### 4.3. Silver nanowires

Silver nitrate contributes the greatest cost to the fabrication of an AgNW film, accounting for 30–65% of the cost of the film. There is a large range in the cost analysis of this TC largely due to the range of prices for common chemicals used to produce the nanowire ink (such as ethylene glycol and methanol), many of which can be found at a greatly reduced price from China.

##### 4.4. Carbon nanotubes

Carbon nanotubes are an extremely expensive material; however, it has often been suggested that this would not necessarily lead to a high cost of SWCNT films since only small amounts are used [66,67]. This study contradicts this assumption and found that carbon nanotubes account for 69% of the cost of the module, even if the cheapest carbon nanotubes currently on the market are used (which have been seen to give inadequate performance in OPV applications [personal communication with X. Wang]). The value for the amount of SWCNTs required in a TC film suggested in [66,67] (approximately 20 mg/m<sup>2</sup>) are based on the amount observed or predicted to be contained within the final film. However, this fails to account for the amount lost during the purification and deposition of the SWCNT ink and a better estimate for the amount of SWCNTs required for the manufacture of a TC is 480 mg/m<sup>2</sup> [personal communication with X. Wang].

A summary of the results of the life cycle and cost analysis are presented in Table 2. The cost of ITO shown in Table 2 is the price offered by manufacturers and thus includes a profit margin and other costs not included in the analysis of other TCs, such as

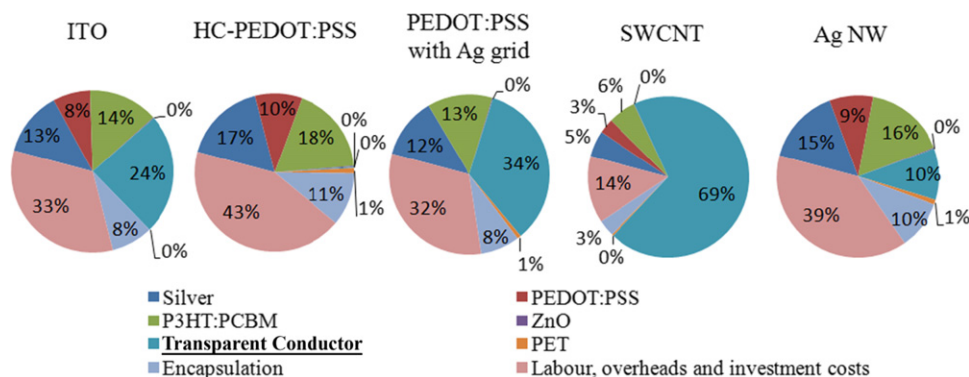


**Fig. 2.** Pie charts show the breakdown on the minimum cost per m<sup>2</sup> of modules using various TCs. Note that the TC in the ITO pie chart includes PET whereas all other TCs include this separately.

labour. These values are therefore an overestimate in comparison to other TCs, which do not include such a margin.

## 5. Effect on module performance

In order to obtain a realistic energy and cost analysis of OPV devices made with ITO-free TCs, their effect on the performance of the solar module should be accounted for.

**Table 3**  
Performance characteristics of TCs, used to provide weightings to performance assumptions.

Transparent conductor	Sheet resistance (Ohms per square)	Transparency	Reference	Weighted efficiency
ITO (baseline)	60.0	79%	[15]	3.00%
HC-PEDOT:PSS	63.3	67%	[16]	2.57%
PEDOT:PSS with Ag grid	–	–	–	Insufficient data
SWCNT	57.0	65%	[48]	2.48%
AgNW	8.0	80%	[20]	3.07%

The sheet resistance of the TC in an OPV device directly influences the Series Resistance,  $R_s$ , across that device, subsequently diminishing the performance of the solar cell. This effect increases with the area of the solar cell such that if an ITO-free electrode is seen to perform equally to an ITO based device in small area solar cells, the same may not be true when large area devices are fabricated [34]. Thus while several articles report ITO-free electrodes performing similarly to ITO reference cells, in small area devices, the higher sheet resistance of the ITO-free electrodes would be expected to degrade performance of large area devices, compared to ITO based devices.

Reduced transparency of the TC in an OPV module will clearly impact its efficiency by reducing the photogenerated current through the device. Many ITO alternatives have a lower sheet resistance with increased thickness but this reduces transparency (e.g. HC-PEDOT:PSS). Thus there is often a need to balance transparency against sheet resistance, which should be considered an important parameter for cell architecture design.

The roughness of TCs, in particular nanowire films, can often cause a reduction in device performance due to increased parasitic current shunting [68], therefore reducing the shunt resistance of the device and deteriorating both the fill factor and the power conversion efficiency [69]. Therefore, an additional layer may be used to prevent shorts across the device. This layer would have its

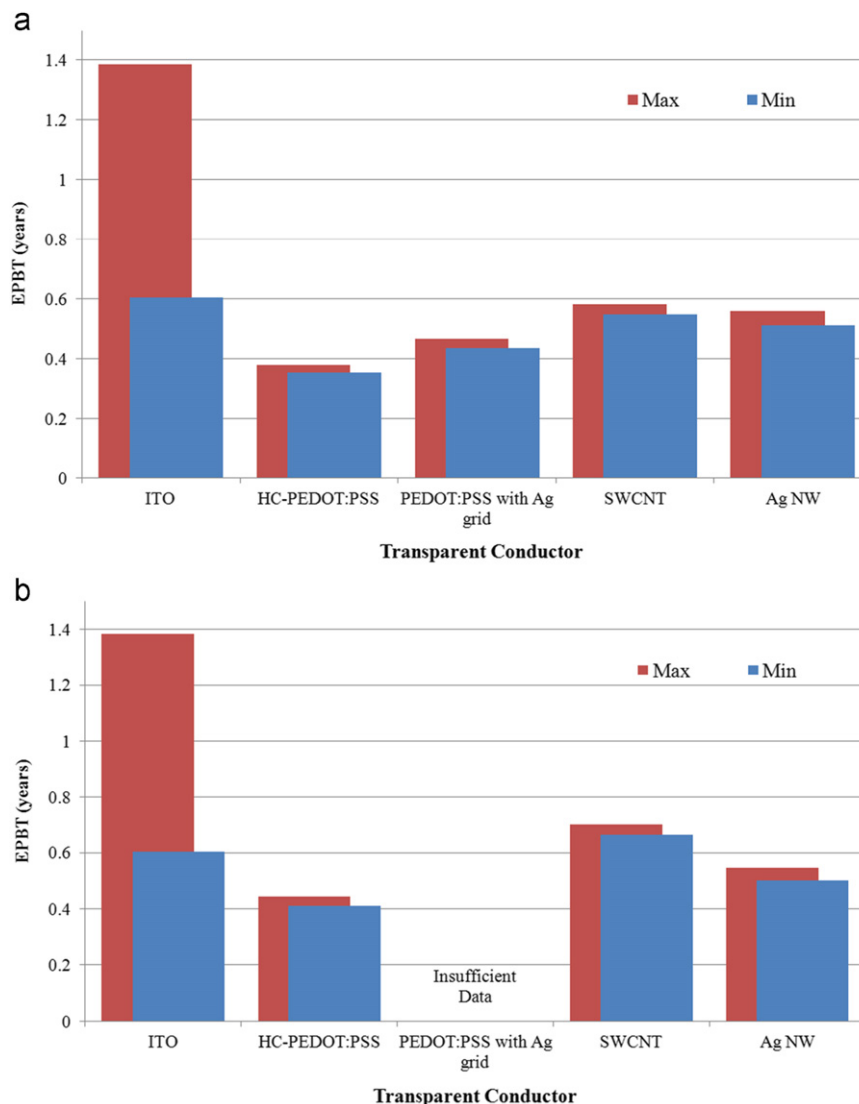


**Fig. 3.** (a) un-weighted and (b) efficiency-weighted EPBT of modules using various TCs.

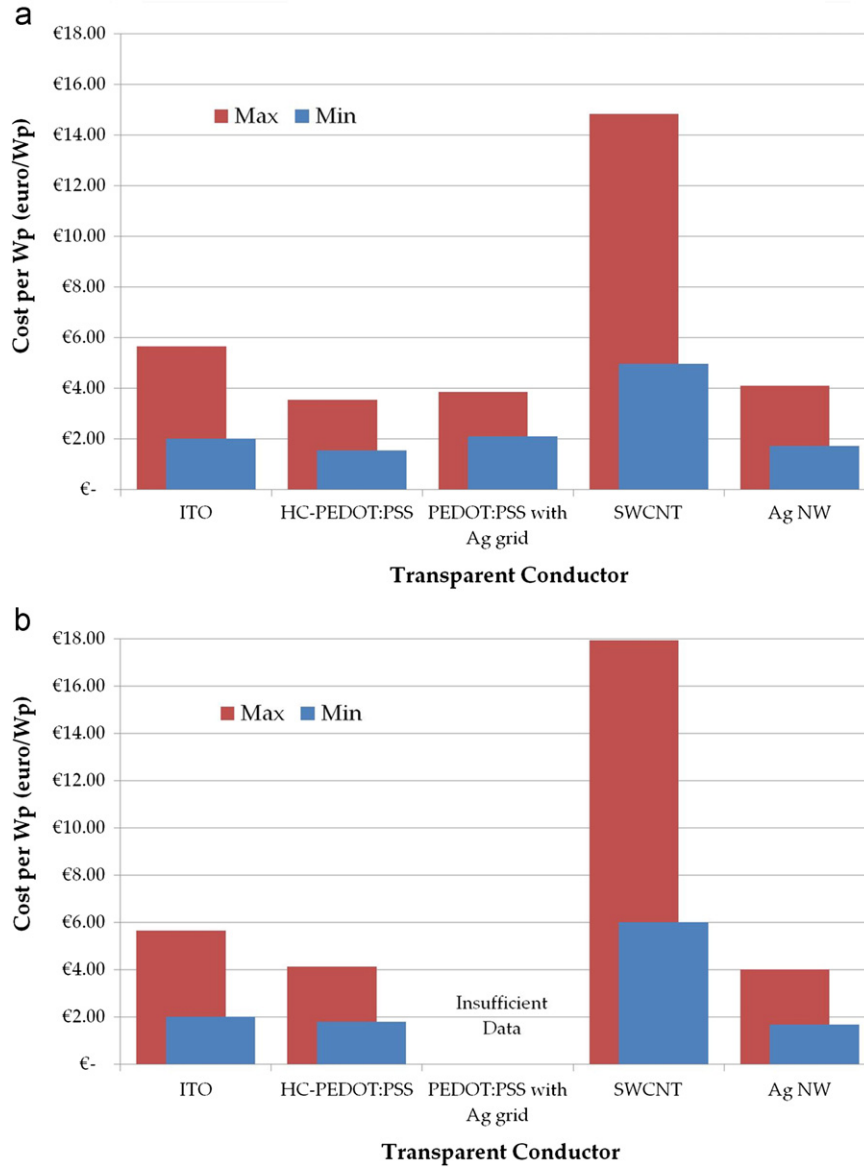


Fig. 4. (a) un-weighted and (b) efficiency-weighted cost per Watt of modules using various TCs.

own environmental, economic and performance cost; however, these are neglected in this study due to lack of reliable data.

The choice of TC can also have a large impact on the lifetime of the module. For example, ITO electrodes are susceptible to ion diffusion into the polymer layers, substantially reducing the efficiency over the lifetime of devices [10]. PEDOT:PSS used as a hole transport layer is often credited as a leading cause of degradation in OPV devices due to the absorption of water by the hydroscopic PEDOT:PSS, which leads to higher resistance in the PEDOT:PSS layer [70]. By utilising PEDOT:PSS as an electrode material, this degradation mechanism would likely be exacerbated since cell performance would be increasingly reliant on the resistance of the PEDOT:PSS layer. This is a major disadvantage to the use of high conductivity polymers as TCs since degradation is already a major issue in organic solar cells. However, effect on the module lifetime of the TC was not accounted for in this study due to insufficient data.

When assessing the EPBT and cost per Watt of OPV modules containing various TCs, the sheet resistance and transparency of the TC was used to assess the expected performance of modules with respect to ITO based devices. TC characteristics of the films prepared using the methods analysed for this study were used

rather than best reported characteristics (which use different methods of fabrication, which may have different LCA results than have been shown in this study). A baseline efficiency was chosen at 3%, corresponding to the use of ITO on a flexible substrate. The difference in performance to the ITO baseline, due to sheet resistance and TC transparency was calculated using Eq. 1, the derivation of which is shown in the supplementary information

$$\eta^{TC} = \frac{T^{TC}}{T^{ITO}} \eta^{ITO} \frac{1 - P_s^{TC}}{1 - P_s^{ITO}} \quad (1)$$

where

$$P_s^{TC} = \frac{b^2}{P_{in}} R_s^{TC} \left[ \frac{T^{TC}}{T^{ITO}} J^{ITO} \right]^2 \quad \text{and} \quad P_s^{ITO} = \frac{b^2}{P_{in}} R_s^{ITO} [J^{ITO}]^2$$

in these expressions:  $\eta^{TC}$  is the weighted efficiency of a cell containing a given TC;  $\eta^{ITO}$  is the baseline, ProcessOne cell efficiency, set at 3%;  $T$  is the transparency of the TC (see Table 3);  $P_s$  is the fractional power loss due to the sheet resistance of the TC;  $J^{ITO}$  is the photogenerated current density in a ProcessOne cell, taken to be 73.3 A/m<sup>2</sup> [1];  $b$  is the width of the cell stripe within the module,

taken to be 6 mm [1];  $R_s$  is the sheet resistance of the TC (see Table 3);  $P_{in}$  is the incident light in test conditions, set at 1000 W/m<sup>2</sup>.

This provides a weighting, shown in Table 3, which was used to compare the TCs. The corresponding effects on the EPBT and cost per Watt are shown in Figs. 3b and 4b, respectively, calculated using the same inputs for active area, insolation and performance ratio as before. A lack of information on other impacts on module performance or lifetime, such as TC roughness or degradation mechanisms, means that these factors could not be quantitatively taken into account.

Insufficient data were available for the composite PEDOT:PSS and silver grid to calculate a theoretical performance weighting for this module. However, a large area module, manufactured similar to ProcessOne has been demonstrated to achieve an efficiency of 0.27% [38]. Using this efficiency, the EPBT was found to be around 5 years and the cost per Watt was found to be between 16.09 €/W<sub>p</sub> and 33.33 €/W<sub>p</sub>.

## 6. Conclusion

A review of the literature shows that there are a number of promising alternatives to ITO, which may be used to reduce the EPBT or financial cost of OPVs in the future. Despite inferior performance by many of these alternatives, the gains made in reduced embodied energy, lower cost and increased flexibility may mean that they still present an attractive alternative. However, the effect on the lifetime due to replacing ITO, has not been assessed here and this may show that the use of materials such as HC-PEDOT:PSS may lead to a reduced lifetime. Some effects on efficiency have also not been considered in this study, such as roughness, which may show that the use of materials such as silver nanowires or carbon nanotubes may result in a higher EPBT or cost than estimated here.

The most promising TCs from an environmental viewpoint are shown to be those based on silver nanowires as well as HC-PEDOT:PSS. However, whilst the high embodied energy in carbon nanotubes does not lead a high embodied energy in SWCNT films, their high economic cost shows that carbon nanotube films will only become competitive if the cost of carbon nanotubes drops significantly or methods of manufacture can reduce the amount of nanotubes discarded during production.

Silver nanowires and HC-PEDOT:PSS both prove to be excellent alternatives to ITO, which have the potential to reduce module costs per Watt by 17% and 10%, and EPBTs by 17% and 32%, with respect to ITO based modules. However, both these materials have a number of potential issues: silver nanowire films may deteriorate performance due to their surface roughness and also have issues with their adhesion to the substrate; whilst HC-PEDOT:PSS may detrimentally affect the lifetime of modules.

## Acknowledgements

The authors would like to thank Xuhua Wang and Monika Voigt for their helpful insights into the use of PEDOT and carbon nanotubes in optoelectronics. In addition, the authors wish to thank EPSRC Pathway to Impact under Grant EP/I50105, MICINN-Spain (HOPE CSD2007-00007; MAT2010-21267-C02) and CARM-Murcia (D429-2008). Jenny Nelson acknowledges the support of the Royal Society through an Industrial Fellowship.

## References

[1] F.C. Krebs, S.A. Gevorgyan, J. Alstrup, A roll-to-roll process to flexible polymer solar cells: model studies, manufacture and operational stability studies, *Journal of Materials Chemistry* 19 (2009) 5442–5451.

[2] A.J. Moule, Power from plastic, *Current Opinion in Solid State & Materials Science* 14 (2010) 123–130.

[3] A. Kumar, C. Zhou, The race to replace tin-doped indium oxide: which material will win? *ACS Nano* 4 (2010) 11–14.

[4] D.S. Hecht, L. Hu, G. Irvin, Emerging transparent electrodes based on thin films of carbon nanotubes, graphene, and metallic nanostructures, *Advanced Materials* 23 (2011) 1482–1513.

[5] R. García-Valverde, J.A. Cherni, A. Urbina, Life cycle analysis of organic photovoltaic technologies, *Progress in Photovoltaics* 18 (2010) 535–558.

[6] Ecoinvent, <www.ecoinvent.ch>, accessed on 15th May 2011.

[7] N. Espinosa, R. García-Valverde, A. Urbina, F.C. Krebs, A life cycle analysis of polymer solar cell modules prepared using roll-to-roll methods under ambient conditions, *Solar Energy Materials and Solar Cells* 95 (2010) 1293–1302.

[8] B. Azzopardi, C.J.M. Emmott, A. Urbina, F.C. Krebs, J. Mutale, J. Nelson, Economic assessment of solar electricity production from organic-based photovoltaic modules in a domestic environment, *Energy and Environmental Science* (2011), doi:10.1039/C1EE01766G.

[9] Critical Raw Materials for the EU: Report of the Ad-hoc Working Group on Defining Critical Raw Materials, in, European Commission, 2010.

[10] A. Andersson, N. Johansson, P. Broms, N. Yu, D. Lupo, W.R. Salaneck, Fluorine tin oxide as an alternative to indium tin oxide in polymer LEDs, *Advanced Materials* 10 (1998) 859–863.

[11] A. Anctil, C. Babbitt, B. Landi, R.P. Raffaele, Life-cycle assessment of organic solar cell technologies, in: *Proceedings of the Photovoltaic Specialists Conference (PVSC), 2010 35th IEEE*, 2010, pp. 000742–000747.

[12] N. Espinosa, R. Garcia-Valverde, F.C. Krebs, Life-cycle analysis of product integrated polymer solar cells, *Energy & Environmental Science* (2011) 1547–1557.

[13] Personal Communication with N. Espinosa and R. García-Valverde.

[14] A.L. Roes, E.A. Alsema, K. Blok, M.K. Patel, Ex-ante environmental and economic evaluation of polymer photovoltaics, *Progress in Photovoltaics* 17 (2009) 372–393.

[15] Sigma-Aldrich, <www.sigmaaldrich.com>, accessed on 1st May 2011.

[16] S.-I. Na, B.-K. Yu, S.-S. Kim, D. Vak, T.-S. Kim, J.-S. Yeo, D.-Y. Kim, Fully spray-coated ITO-free organic solar cells for low-cost power generation, *Solar Energy Materials and Solar Cells* 94 (2010) 1333–1337.

[17] M. Fabretto, J.P. Autere, D. Hoglinger, S. Field, P. Murphy, Vacuum vapour phase polymerised poly(3,4-ethylenedioxythiophene) thin films for use in large-scale electrochromic devices, *Thin Solid Films* 519 (2011) 2544–2549.

[18] Y. Galagan, J.-E.J.M. Rubingh, R. Andriessen, C.-C. Fan, P.W.M. Blom, S.C. Venstra, J.M. Kroon, ITO-free flexible organic solar cells with printed current collecting grids, *Solar Energy Materials and Solar Cells* 95 (2011) 1339–1343.

[19] M.G. Kang, M.S. Kim, J.S. Kim, L.J. Guo, Organic solar cells using nanoimprinted transparent metal electrodes (vol. 20, p. 4408, 2008), *Advanced Materials* 20 (2008) 4408–4413.

[20] L.B. Hu, H.S. Kim, J.Y. Lee, P. Peumans, Y. Cui, Scalable coating and properties of transparent, flexible, silver nanowire electrodes, *ACS Nano* 4 (2010) 2955–2963.

[21] S. De, T.M. Higgins, P.E. Lyons, E.M. Doherty, P.N. Nirmalraj, W.J. Blau, J.J. Boland, J.N. Coleman, Silver nanowire networks as flexible, transparent, conducting films: extremely high dc to optical conductivity ratios, *ACS Nano* 3 (2009) 1767–1774.

[22] H.-Z. Geng, K.K. Kim, K.P. So, Y.S. Lee, Y. Chang, Y.H. Lee, Effect of acid treatment on carbon nanotube-based flexible transparent conducting films, *Journal of the American Chemical Society* 129 (2007) 7758–7759.

[23] S. Bae, H. Kim, Y. Lee, X.F. Xu, J.S. Park, Y. Zheng, J. Balakrishnan, T. Lei, H.R. Kim, Y.I. Song, Y.J. Kim, K.S. Kim, B. Ozyilmaz, J.H. Ahn, B.H. Hong, S. Iijima, Roll-to-roll production of 30-inch graphene films for transparent electrodes, *Nature Nanotechnology* 5 (2010) 574–578.

[24] H.X. Chang, G.F. Wang, A. Yang, X.M. Tao, X.Q. Liu, Y.D. Shen, Z.J. Zheng, A. Transparent, Flexible, low-temperature, and solution-processible graphene composite electrode, *Advanced Functional Materials* 20 (2010) 2893–2902.

[25] P.A. Levermore, L.C. Chen, X.H. Wang, R. Das, D.D.C. Bradley, Highly conductive poly(3,4-ethylenedioxythiophene) films by vapor phase polymerization for application in efficient organic light-emitting diodes, *Advanced Materials* 19 (2007) 2379–2385.

[26] S.K.M. Jönsson, J. Birgersson, X. Crispin, G. Greczynski, W. Osikowicz, A.W. Denier van der Gon, W.R. Salaneck, M. Fahlman, The effects of solvents on the morphology and sheet resistance in poly(3,4-ethylenedioxythiophene)-polystyrenesulfonic acid (PEDOT-PSS) films, *Synthetic Metals* 139 (2003) 1–10.

[27] B.Y. Ouyang, C.W. Chi, F.C. Chen, Q.F. Xi, Y. Yang, High-conductivity poly(3,4-ethylenedioxythiophene): poly(styrene sulfonate) film and its application in polymer optoelectronic devices, *Advanced Functional Materials* 15 (2005) 203–208.

[28] E. Ahlswede, W. Muhleisen, M. Wahi, J. Hanisch, M. Powalla, Highly efficient organic solar cells with printable low-cost transparent contacts, *Applied Physics Letters* 92 (2008) 143307-1–143307-3.

[29] H. Do, M. Reinhard, H. Vogeler, A. Puetz, M.F.G. Klein, W. Schabel, A. Colmann, U. Lemmer, Polymeric anodes from poly(3,4-ethylenedioxythiophene):poly(styrenesulfonate) for 3.5% efficient organic solar cells, *Thin Solid Films* 517 (2009) 5900–5902.

[30] S.K. Hau, H.-L. Yip, J. Zou, A.K.Y. Jen, Indium tin oxide-free semi-transparent inverted polymer solar cells using conducting polymer as both bottom and top electrodes, *Organic Electronics* 10 (2009) 1401–1407.

- [31] Y.H. Kim, C. Sachse, M.L. Machala, C. May, L. Müller-Meskamp, K. Leo, Highly conductive PEDOT:PSS electrode with optimized solvent and thermal post-treatment for ITO-free organic solar cells, *Advanced Functional Materials* 21 (2011) 1076–1081.
- [32] J.R. Kim, J.M. Cho, W.S. Shin, W.W. So, S.J. Moon, Analysis of ITO-free organic solar cells using a highly conductive polymer anode, *Molecular Crystals and Liquid Crystals* 519 (2010) 245–251.
- [33] S.-I. Na, S.-S. Kim, J. Jo, D.-Y. Kim, Efficient and flexible ITO-free organic solar cells using highly conductive polymer anodes, *Advanced Materials* 20 (2008) 4061–4067.
- [34] J.S. Yeo, J.M. Yun, S.S. Kim, D.Y. Kim, J. Kim, S.I. Na, Variations of cell performance in ITO-free organic solar cells with increasing cell areas, *Semiconductor Science and Technology* 26 (2011) 034010-1–034010-6.
- [35] Y.H. Zhou, F.L. Zhang, K. Tvingstedt, S. Barrau, F.H. Li, W.J. Tian, O. Inganäs, Investigation on polymer anode design for flexible polymer solar cells, *Applied Physics Letters* 92 (2008) 233308-1–233308-3.
- [36] P.A. Levermore, R. Jin, X.H. Wang, L.C. Chen, D.D.C. Bradley, J.C. de Mello, High efficiency organic light-emitting diodes with PEDOT-based conducting polymer anodes, *Journal of Materials Chemistry* 18 (2008) 4414–4420.
- [37] T. Aernouts, P. Vanlaeke, W. Geens, J. Poortmans, P. Heremans, S. Borghs, R. Mertens, R. Andriessen, L. Leenders, Printable anodes for flexible organic solar cell modules, *Thin Solid Films* 451–452 (2004) 22–25.
- [38] F.C. Krebs, All solution roll-to-roll processed polymer solar cells free from indium-tin-oxide and vacuum coating steps, *Organic Electronics* 10 (2009) 761–768.
- [39] B. Zimmermann, H.-F. Schleiermacher, M. Niggemann, U. Würfel, ITO-free flexible inverted organic solar cell modules with high fill factor prepared by slot die coating, *Solar Energy Materials and Solar Cells* 95 (2011) 1587–1589.
- [40] J.Y. Zou, H.L. Yip, S.K. Hau, A.K.Y. Jen, Metal grid/conducting polymer hybrid transparent electrode for inverted polymer solar cells, *Applied Physics Letters* 96 (2010) 203301-1–203301-3.
- [41] S.H. Ahn, L.J. Guo, High-speed roll-to-roll nanoimprint lithography on flexible plastic substrates, *Advanced Materials* 20 (2008) 2044–2049.
- [42] S.H. Ahn, L.J. Guo, Large-area roll-to-roll and roll-to-plate nanoimprint lithography: a step toward high-throughput application of continuous nanoimprinting, *ACS Nano* 3 (2009) 2304–2310.
- [43] M.G. Kang, T. Xu, H.J. Park, X.G. Luo, L.J. Guo, Efficiency enhancement of organic solar cells using transparent plasmonic Ag nanowire electrodes, *Advanced Materials* 22 (2010) 4378–4383.
- [44] J.Y. Lee, S.T. Connor, Y. Cui, P. Peumans, Solution-processed metal nanowire mesh transparent electrodes, *Nano Letters* 8 (2008) 689–692.
- [45] W. Gaynor, J.Y. Lee, P. Peumans, Fully solution-processed inverted polymer solar cells with laminated nanowire electrodes, *ACS Nano* 4 (2010) 30–34.
- [46] A.R. Madaria, A. Kumar, F.N. Ishikawa, C.W. Zhou, Uniform, highly conductive, and patterned transparent films of a percolating silver nanowire network on rigid and flexible substrates using a dry transfer technique, *Nano Research* 3 (2010) 564–573.
- [47] X.Y. Zeng, Q.K. Zhang, R.M. Yu, C.Z. Lu, A new transparent conductor: silver nanowire film buried at the surface of a transparent polymer, *Advanced Materials* 22 (2010) 4484–4488.
- [48] S. Kim, J. Yim, X. Wang, D.D.C. Bradley, S. Lee, J.C. Demello, Spin- and spray-deposited single-walled carbon-nanotube electrodes for organic solar cells, *Advanced Functional Materials* 20 (2010) 2310–2316.
- [49] S.-G. Ihn, K.-S. Shin, M.-J. Jin, X. Bulliard, S. Yun, Y.S. Choi, Y. Kim, J.-H. Park, M. Sim, M. Kim, K. Cho, T.S. Kim, D. Choi, J.-Y. Choi, W. Choi, S.-W. Kim, ITO-free inverted polymer solar cells using a GZO cathode modified by ZnO, *Solar Energy Materials and Solar Cells* 95 (2011) 1610–1614.
- [50] J. Meiss, M.K. Riede, K. Leo, Towards efficient tin-doped indium oxide (ITO)-free inverted organic solar cells using metal cathodes, *Applied Physics Letters* 94 (2009) 013303-1–013303-3.
- [51] J. Ajuria, I. Etxebarria, W. Cambarau, U. Munecas, R. Tena-Zaera, J.C. Jimeno, R. Pacios, Inverted ITO-free organic solar cells based on p and n semiconducting oxides. New designs for integration in tandem cells, top or bottom detecting devices, and photovoltaic windows, *Energy & Environmental Science* 4 (2011) 453–458.
- [52] H.M. Stec, R.J. Williams, T.S. Jones, R.A. Hatton, Ultrathin Transparent Au Electrodes for organic photovoltaics fabricated using a mixed mono-molecular nucleation layer, *Advanced Functional Materials* 21 (2011) 1709–1716.
- [53] T.H. Reilly, J. van de Lagemaat, R.C. Tenent, A.J. Morfa, K.L. Rowlen, Surface-plasmon enhanced transparent electrodes in organic photovoltaics, *Applied Physics Letters* 92 (2008) 243304-1–243304-3.
- [54] L.G. De Arco, Y. Zhang, C.W. Schlenker, K. Ryu, M.E. Thompson, C.W. Zhou, Continuous, highly flexible, and transparent graphene films by chemical vapor deposition for organic photovoltaics, *ACS Nano* 4 (2010) 2865–2873.
- [55] M. Choe, B.H. Lee, G. Jo, J. Park, W. Park, S. Lee, W.K. Hong, M.J. Seong, Y.H. Kahng, K. Lee, T. Lee, Efficient bulk-heterojunction photovoltaic cells with transparent multi-layer graphene electrodes, *Organic Electronics* 11 (2010) 1864–1869.
- [56] A. Ismach, C. Druzgalski, S. Penwell, A. Schwartzberg, M. Zheng, A. Javey, J. Bokor, Y. Zhang, Direct chemical vapor deposition of graphene on dielectric surfaces, *Nano Letters* 10 (2010) 1542–1548.
- [57] C. Mattevi, H. Kim, M. Chhowalla, A review of chemical vapour deposition of graphene on copper, *Journal of Materials Chemistry* 21 (2011) 3324–3334.
- [58] V.P. Verma, S. Das, I. Lahiri, W. Choi, Large-area graphene on polymer film for flexible and transparent anode in field emission device, *Applied Physics Letters* 96 (2010) 203103–203108.
- [59] Y. Wang, X.H. Chen, Y.L. Zhong, F.R. Zhu, K.P. Loh, Large area, continuous, few-layered graphene as anodes in organic photovoltaic devices, *Applied Physics Letters* 95 (2009) 063302-1–063302-3.
- [60] G. Kalita, M. Matsushima, H. Uchida, K. Wakita, M. Umeno, Graphene constructed carbon thin films as transparent electrodes for solar cell applications, *Journal of Materials Chemistry* 20 (2010) 9713–9717.
- [61] M. Held, M. Shibasaki, SENSE—LCA Results, University of Stuttgart, 2008.
- [62] Z.Y. Yin, S.Y. Sun, T. Salim, S.X. Wu, X.A. Huang, Q.Y. He, Y.M. Lam, H. Zhang, Organic photovoltaic devices using highly flexible reduced graphene oxide films as transparent electrodes, *ACS Nano* 4 (2010) 5263–5268.
- [63] J.B. Wu, H.A. Becerril, Z.N. Bao, Z.F. Liu, Y.S. Chen, P. Peumans, Organic solar cells with solution-processed graphene transparent electrodes, *Applied Physics Letters* 92 (2008) 263302-1–263302-3.
- [64] D. Zhang, K. Ryu, X. Liu, E. Polikarpov, J. Ly, M.E. Thompson, C. Zhou, Transparent, conductive, and flexible carbon nanotube films and their application in organic light-emitting diodes, *Nano Letters* 6 (2006) 1880–1886.
- [65] D. Kushnir, B.A. Sanden, Energy requirements of carbon nanoparticle production, *Journal of Industrial Ecology* 12 (2008) 360–375.
- [66] K.A. Sierros, D.S. Hecht, D.A. Banerjee, N.J. Morris, L. Hu, G.C. Irvin, R.S. Lee, D.R. Cairns, Durable transparent carbon nanotube films for flexible device components, *Thin Solid Films* 518 (2010) 6977–6983.
- [67] R.C. Tenent, T.M. Barnes, J.D. Bergeson, A.J. Ferguson, B. To, L.M. Gedvilas, M.J. Heben, J.L. Blackburn, Ultrasoft, large-area, high-uniformity, conductive transparent single-walled-carbon-nanotube films for photovoltaics produced by ultrasonic spraying, *Advanced Materials* 21 (2009) 3210–3216.
- [68] B. O'Connor, C. Haughn, K.H. An, K.P. Pipe, M. Shtein, Transparent and conductive electrodes based on unpatterned, thin metal films, *Applied Physics Letters* 93 (2008) 223304-1–223304-3.
- [69] J. Nelson, *The Physics of Solar Cells*, Imperial College Press, 2003.
- [70] K. Kawano, R. Pacios, D. Poplavskyy, J. Nelson, D.D.C. Bradley, J.R. Durrant, Degradation of organic solar cells due to air exposure, *Solar Energy Materials and Solar Cells* 90 (2006) 3520–3530.